 doi:10.20944/preprints202104.0563.v1

*Article*

# Fabrication of micron scale three-dimensional single crystal diamond channel: by micro-jet water-assist laser

**Qiang Wei [1#], Xiaofan Zhang [1#], Fang Lin [1], ,Ruozheng Wang [1], Genqiang Chen [1] and Hong-Xing Wang [1*]**

1 Key Laboratory of Physical Electronics and Devices, Ministry of Education, School of Electronic Science and Engineering, Xi'an Jiaotong University, Xi'an, 710049, China
# These two authors contributed equally to this study and share the first authorship
* Correspondence: hxwangcn@xjtu.edu.cn

**Abstract:** Two types of trenches cross-section in conventional vertical and brand new reverse-V-shape have fabricated on SCD substrate by micro-jet water-assist laser, the epitaxial lateral overgrowth technique has applied by microwave plasma chemical vapor deposition system in forming multiple micrometer-size channels. Raman and SEM techniques have applied in analyze both types growth layer characterization. Optical microscope has used to test microchannels hollowness. As a result, with the brand new reverse-V-shape trench, epitaxial lateral overgrowth layer reaches higher SCD surface morphology and crystal quality.

**Keywords:** Single crystal diamond; micro-water jet guided laser; microchannel

## 1. Introduction

Diamond, one of the most promising material, has brought lots of attention to researchers in electronic process thermal management, because of its stable chemical properties, high-temperature operation and low friction coefficient of thermal expansion. In addition, diamond has super hard wearing resistance and has 2000-2600 W/m•k thermal conductivity [1,2]. Diamond with microchannel is ideal substrate in cooling chip temperature and achieve low thermal resistance [3,4]; in enlarging surface and heat exchange areas of catalytic elements; and in assisting liquid pass through as a stent in medical equipment area. Therefore, The wilder of diamond microchannel application, the more important of quality improvement since then.

The most common reported single crystal diamond microchannel fabrication were used ion beam lithography [5] and epitaxial lateral overgrowth techniques [6]. An article of micro-water jet guided laser perpendicular cutting trenches as a feasible way to fabricate single crystal diamond (SCD) microchannel has been reported [7], but the surface quality of that type of microchannel has not been improved and the defects have not been inhibited. Therefore, a better performance microchannel fabrication with an efficiency method is needed.

This research work has carried out a three-dimensional microchannel with fairly large and controllable geometry on SCD substrate. The cross-section of microchannel on SCD substrate is a reverse-V-shape, which has machined by micro-jet water-assist laser. Then, epitaxial lateral overgrowth has applied by microwave plasma chemical vapor deposition system on processed substrate. Optical microscope and scanning electron microscope (SEM) were used to distinguish the difference of growth area and identify growth layer morphology as well as testing channel hollowness. Raman and X-ray diffraction (XRD) techniques were applied in characterization and quality determination. Finally, the growth principles were analyzed in schematic illustration.

## 2. Materials and Methods

Preprints (www.preprints.org) | NOT PEER-REVIEWED | Posted: 21 April 2021 doi:10.20944/preprints202104.0563.v1

The high-pressure high-temperature (HPHT) SCD (1 0 0) substrate was used as the experimental material in the dimensional of 3 mm x 3 mm x 1 mm. The substrate was located on a three dimension X- Y- and Z-axis removable work piece stage of laser system, which contained a Nd:YAG (Neodymium Doped Yttrium Aluminum Garnet) laser, and a 50 W high-power supply. The wavelength of the laser was 532 nm and the focusing system consisted quartz optical lenses, and the water chamber was filled with ultra-pure de-ionized (DI) water. The DI water pressure, nozzle diameter and helium protect gas flow were 400 bar, 50 μm and 1.1 L/min, respectively. The cutting speed was kept constant at 8 mm/s coming from the previous research result.

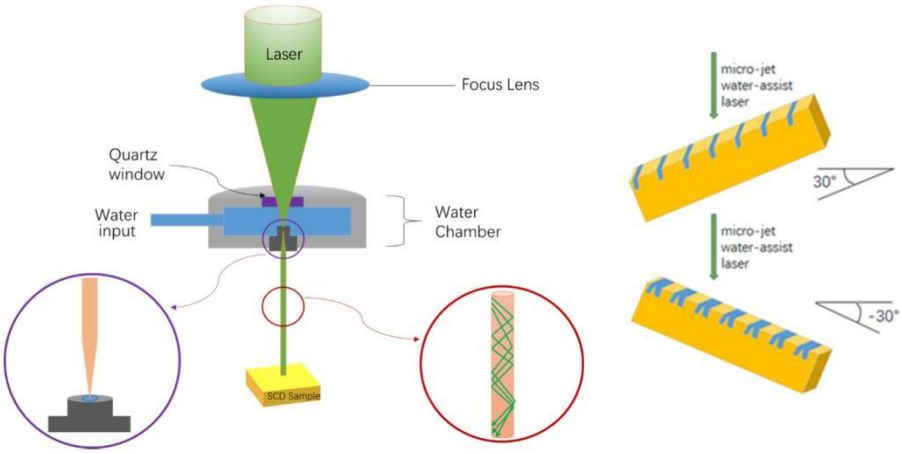


**Figure 1.** Schematic of the micro-jet water-assist laser working principle.

There were two different styles of trenches have brought out, one is conventional one which laser perpendicular to SCD substrate surface cutting indicating an approximate rectangle on cross section. The other is an exploratory trench which the cross section showing a reverse V-shape. In detail, diamond substrate was cut twice by micro-jet water-assist laser and was rotated twice in a certain degree with a sharing opening.

Because SCD substrate trench inner-face was carbonized by laser machining, hydrogen/oxygen plasma and a mixed acid of H2SO4 and HNO3 at 250℃ for 3 hrs were applied to clean the non-diamond phase. The growth conditions were as follows: 950℃ substrate temperature, 500 sccm of H2 flow, 40 sccm of CH4 flow, and gas pressure of 110 Torr. It has taken 10 hrs to reach the desirable as-grown diamond layer and the thickness was about 100μm. The epitaxial lateral overgrowth (ELO) method [8] was applied in helping trenches sidewall merging and forming microchannels. .

## 3. Results and discussion

The SEM images of conventional perpendicular trenches in diamond substrate after laser treatment are shown in Figure 2. It is shown that multiple trenches are parallel and running through diamond surface in Figure 2(a), exhibiting a nice uniformity with clear boundary. The morphology of each trench is identical, which the trench length, top opening width, central width and overall depth are 3mm, 55um, 55um, and 265um respectively as shown in Figure 2(c). The width of the fabricated indicating that the cross section after laser treatment is approximate a rectangle shape with a curvy bottom as shown in Figure 2(c). Figure 2(b) is a cross section SEM image of diamond substrate after epitaxial lateral overgrowth by microwave plasma chemical vapor deposition system, exhibiting the trench top is closed and fully covered by epitaxial lateral overgrowth. The horizontal direction and vertical direction, after merging, growth occurred the entire surface of the substrate crystal, allowing a good quality layer SCD to be obtained. The SEM image of enlarged after growth trench cross section is shown in Figure 2(d), which is notable the top width is decreased to 35 nm, however, the central width kept as 55 nm. Base on the observations, we calculated the opening width has shrunk by 36%. After 10 hours

Preprints (www.preprints.org) | NOT PEER-REVIEWED | Posted: 21 April 2021 doi:10.20944/preprints202104.0563.v1

epitaxial lateral overgrowth, the sidewalls of each trench gradually merged into one another during horizontal and vertical growth, indicating the water drop-shaped microchannel has been fabricated and its overall depth is longer than trench depth.

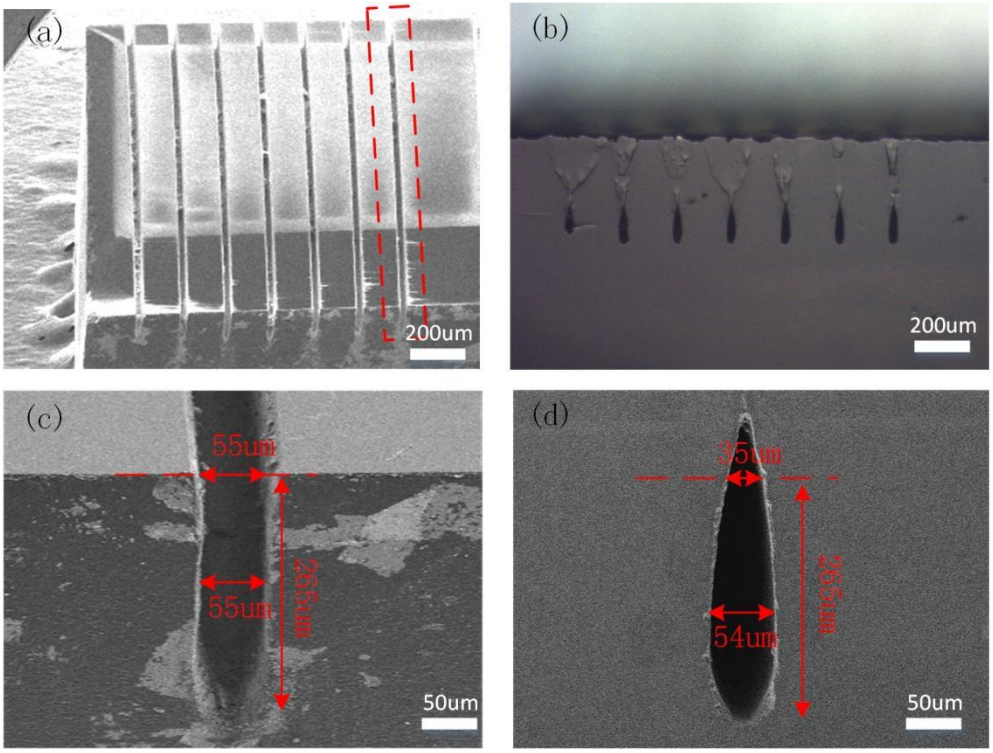


**Figure 2.** Cross section SEM image of SCD substrate (a)after laser treatment(45°); (b) after epitaxial lateral diamond overgrowth; (c) Enlarged view of trenches; (d)Enlarged view of (b).

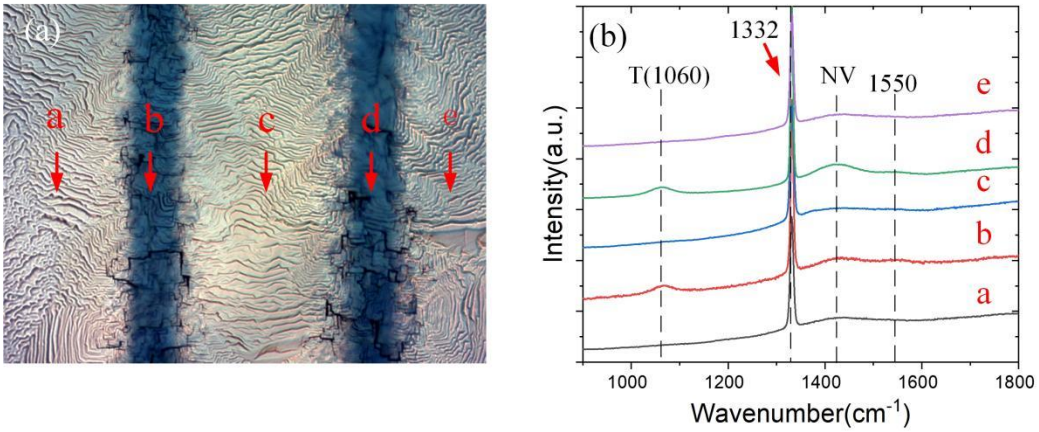


**Figure 3.** (a)After growth of the image; (b) Raman spectra taken from different locations around the channel (as shown in the adjacent images).

In order to investigate the morphologies around the microchannel, the optical microscope image was taken under back-light as shown in Figure 3(a), which the dark stripes representing microchannels and the light area indicating Homoepitaxial growth. In order to study the composition around the channel, Raman measurements were performed in the position (a-e) indicated on the substrate after growth optical microscope image . The Raman excitation wavelength was 532 nm. It shows a strong peak at 1332 cm-1 in all five (a-e) regions, indicating a good composition of single crystal diamond [9] as shown in Figure 3(b). As meanwhile, a peak located in Raman spectra at 1430-1470 cm-1, a slight

Preprints (www.preprints.org) | NOT PEER-REVIEWED | Posted: 21 April 2021 doi:10.20944/preprints202104.0563.v1

N photoluminescence peaks appearing in the position of a, c and e. Raman spectra in microchannel (position b and d) are approaching sp3 carbon peak at 1060cm$^{-1}$ [10], as well as that of sp2 amorphous carbon peak located at 1550 cm-1can be observed [11]. These suggest that amorphous carbon was first formed on microchannel position and some sp3 hybridization carbon mixed up with sp2 amorphous carbon [12].

Figure 4(a) shows schematic diagram of formation of reverse V-shape trench. The flat HPHT SCD substrate was rotated 30° to vertical direction to get the first tilted channel by micro-water jet guided laser and then rotated -30° to get the second channel with sharing the top opening. Following the cutting procedure the substrate was submitted to acid cleaning in order to remove all graphite residues and flaws left by laser treatment. The growth of substrate was carried out by epitaxial lateral overgrowth by microwave plasma chemical vapor deposition system as same condition as conventional perpendicular trenches. The SEM image of cross section after-growth, which is noticeable that reverse V-shape trench top opening completely disappeared, leaving a triangle shape and closed surface free of any defects, as shown in Figure 4(b). The top opening width was decreased from 74um to 69 um, which was calculated shrinking by 7% and lateral growth was effectively inhibited. The trench top gradually closed during horizontal and vertical growth merging, indicating the overall depth is longer than before growth and all the trenches formed reverse V-shape microchannel.

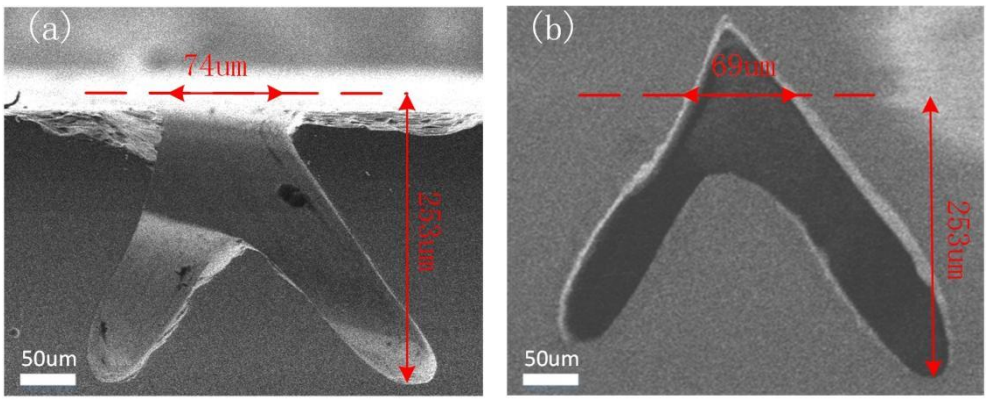


**Figure 4.** (a)SEM of reverse-V-shape microchannel; (b) After growth.

The after-growth surface optical microscope image of reverse-V-shape microchannel after growth is shown in Figure 5a revealing a fairly larger dark stripe than that of conventional vertical channel. Both dark and light regions appear consistent morphology of single crystal diamond characterization. Raman spectra in 532 nm excitation wavelength was applied to investigate the crystal composition around microchannel, which position a-c were marked as shown in Figure 5b. It shows a very week N photoluminescence peak at 1430-1470 cm-1 besides a strong peak at 1332 cm-1 in a and c positions. However, a slight sp3 hybridization carbon peak at 1060cm-1 and barely sp2 amorphous carbon peak at 1550 cm-1 can be observed in position b. These phenomena indicate homoepitaxial after-growth surface quality has not affected by applying reverse-V-shape microchannel.

Preprints (www.preprints.org) | NOT PEER-REVIEWED | Posted: 21 April 2021 doi:10.20944/preprints202104.0563.v1

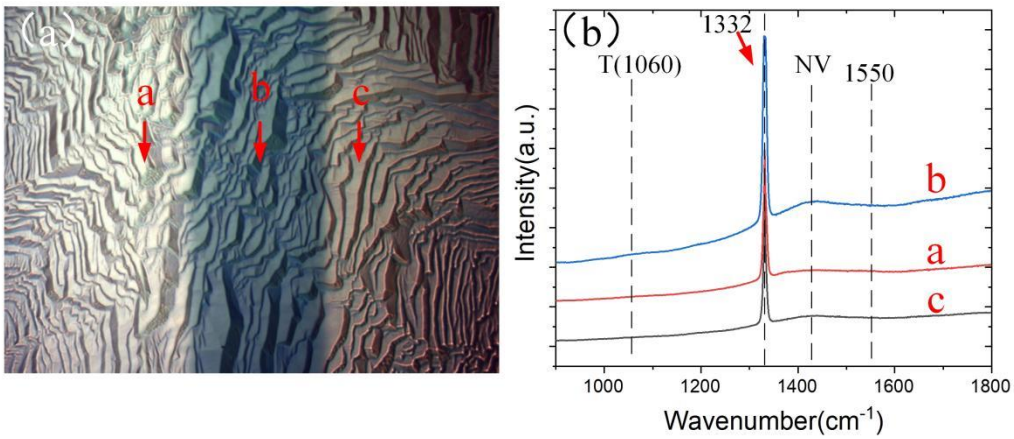


**Figure 5.** (a)After growth of the image; (b)Raman spectra taken from different locations around the channel(as shown in the adjacent images).

To evaluate and compare the quality of substrate and after growth films of two different microchannel types, XRD technique has been carried out as shown in Figure 6. The full widths at half maximum value of substrate is 0.015° (figure 6(a)) and that of epitaxial lateral overgrowth film of conventional vertical microchannel and reverse-V-shape microchannel are 0.042° and 0.031° respectively whose spectra are present in Figure 6 (b) and (c). It is noticeable that the quality of epitaxial lateral overgrowth value of reverse-V-shape cutting strategy is better than of conventional vertical microchannel, and it's comparable to the substrate, revealing an acceptable quality.

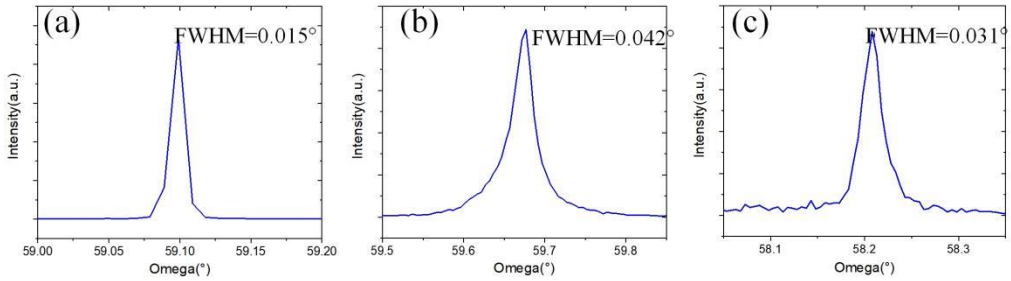


**Figure 6.** XRD Scanning (a)SCD substrate; (b)vertical microchannel; (c)reverse-V-shape microchannel.

Eventually, the principle of growing difference of each type microchannel is analyzed, which the schematic diagram of conventional vertical trench and reverse-V-shape growth status are shown in Figure 7 (a) and (b), respectively. At the growth stage, reaction gas penetrated into microchannel and interacted with channel inter-wall forming single crystal diamond. It is noticeable that the reaction gas concentration decreased with channel depth increasing. Because of two types of cutting strategy, the cross section of conventional vertical microchannel revealing smaller cavity area than that of reverse-V-shape. Therefore, the concentration of reaction gas into inter-wall of two type microchannels are much different, which the conventional vertical microchannel has more concentrated growing environment in SCD forming and inward expanding. The reverse-V-shape microchannel central and bottom area barely interact with gas and restraining defect. Because the channel inter-wall was rough and with amorphous diamond after laser cutting, therefore, some flaws and defects start to arise and affect lateral growing quality. For compare and contrast, reverse-V-shape microchannel is better choice to applied in improving microchannel top surface quality and inhibiting the extended defects.

Preprints (www.preprints.org) | NOT PEER-REVIEWED | Posted: 21 April 2021 doi:10.20944/preprints202104.0563.v1

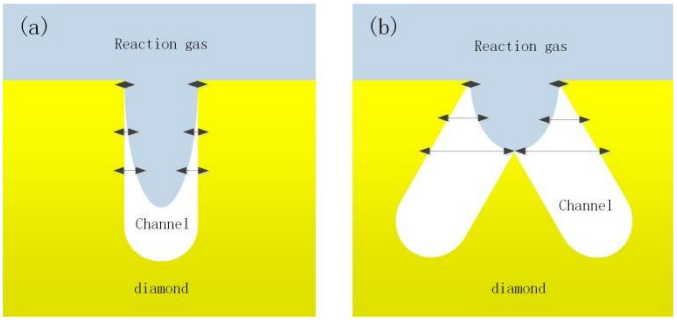


**Figure 7.** Two types microchannel (a)vertical trench; (b)reverse-V-shape trench.

Figure 8 (a) shows the optical microscope image of reverse-V-shape microchannel cross section, which can be observed clearly with nice boundary under white backlight. To check the hollowness and continuity, as shown in Figure 7 (b), cross section optical microscope image of its microchannel with red backlight from front side and backside were applied, indicating that microchannel were and coherence and continuous.

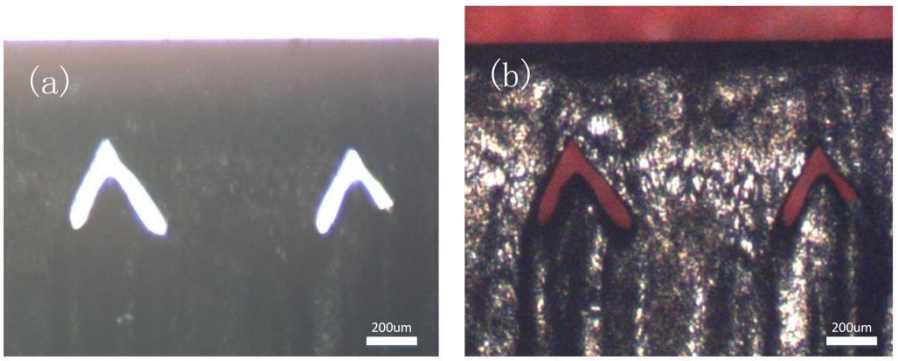


**Figure 8.** Cross section optical microscope images of SCD microchannels with various backlight from (a)white light; (b)red light.

## 4. Conclusions

In summary, reverse-V-shape three-dimensional microchannels in single crystal diamond have been fully carried out. The first step of micro trenches were fabricated by micro-jet assisted laser cutting technique and the second step of microchannels were fabricated by epitaxial lateral overgrowth technique. The optical microscope and SEM images show that morphologies and structures for microchannel formation. Raman and XRD spectra were used to evaluate after growth crystal characteristics, appearing an acceptable single crystal diamond quality. Schematic illustrate the advantage of reverse-V-shape microchannel in inhibiting diamond growth defects compares to co nventional vertical microchannel. The coherence and hollowness were checked of reverse-V-shape microchannel under two colors of backlight, indicating its consistency and continuity. This work could provide a controllable process to fabricate single crystal diamond heat sink and applied in high power devices.

**Author Contributions:** Qiang Wei designed and invested the research. Xiaofan Zhang carried out the experiments. Fang Lin and Ruozheng Wang grew and diamond films. Genqiang Chen analyzed the results. Hong-Xing Wang reviewed the manuscript.

**Funding:** This research was funded by National Key Research and Development Program of China (Grant No. 2018YFE0125900), National Natural Science Foundation of China (Grant No. 61627812, 61804122), China Postdoctoral Science Foundation (Grant No. 2019M653637, 2019M660256, 2020M683485).

**Conflicts of Interest:** The authors declare no conflict of interest.

## References


1. May, P. W. Materials science. The new diamond age [J]. *Science* **2008**, *319*, 1490-1.
2. Isberg, J.; Hammersberg, J.; Bernhoff, H. et al. Charge collection distance measurements in single and polycrystalline CVD diamond [J]. *Diamond & Related Materials* **2004**, *13*, 872-875.
3. Hetsroni, G.; Mosyak, A.; Pogrebnyak, E. et al. Fluid flow in micro-channels [J]. *International Journal of Heat & Mass Transfer* **2005**, 48, 1982-1998.
4. Anthony, T. R.; Banholzer, W. F.; Fleisher, J. F. et al. Thermal diffusivity of isotopically enriched 12C diamond [J]. *Physical review. B, Condensed matter* **1990**, 42, 1104-1111.
5. Tchernij, S.; Skukan, N.; Picollo, F. et al. Electrical characterization of a graphite-diamond-graphite junction fabricated by MeV carbon implantation [J]. *Diamond & Related Materials* **2017**, 74, 125-131.
6. Fu, J.; Zhu, T. F.; Zhang, M. H. et al. Fabrication of single crystal diamond microchannels for microelectromechanical systems [J]. *Diamond & Related Materials* **2017**:S0925963517303515.
7. Fu, J.; Wang, Y.; Wang, J. et al. Fabrication of hundreds of microns three-dimensional single crystal diamond channel along with high aspect ratio by two-step process [J]. *Materials Letters* **2019**, 255, 126556-126556.
8. Steven, P.J.; Robert, N. Raman spectroscopy of diamond and doped diamond, *Phil. Trans. R. Soc. Lond. A* **2004**, 362, 2537–2565.
9. Gilkes, K. W. et al. Direct quantitative detection of the sp. bonding in diamond-like carbon films using ultraviolet and visible Raman spectroscopy.[J]. *Journal of Applied Physics* **2000.**
10. Ferrari, A. C.; Robertson, J. Origin of the 1150 cm 1 Raman mode in nanocrystalline diamond[J]. *Physical Review B* **2001**, 63, 263-271.
11. Shroder, R. E., Nemanich, R J , Glass, J. T. Analysis of the Composite Structures in Diamond Thin Films by Raman Spectroscopy[J]. *Physical review. B, Condensed matter* **1990**, 41,3738-3745.
12. Yarbrough, W. A.; Messier, R . Current Issues and Problems in the Chemical Vapor Deposition of Diamond [J]. *Science* **1990**, 247, 688-96.